

Quasiclassical Trajectory Calculations of Acetaldehyde Dissociation on a Global Potential Energy Surface Indicate Significant Non-transition State Dynamics

Benjamin C. Shepler,[†] Bastiaan J. Braams,[‡] and Joel M. Bowman^{*,†}

Department of Chemistry and Cherry L. Emerson Center for Scientific Computation, and
Department of Mathematics and Computer Science, Emory University, Atlanta, Georgia 30322

Received: June 15, 2007; In Final Form: July 16, 2007

A recent experimental study [Houston, P. L.; Kable, S. H. *Proc. Natl. Acad. Sci. U.S.A.* **2006**, *103*, 16079] of the photodissociation of acetaldehyde (CH_3CHO) has suggested two distinct mechanisms for the production of the molecular products $\text{CH}_4 + \text{CO}$. One corresponds to the traditional transition state mechanism and the other to a transition state-skirting path similar to the roaming channel previously reported in formaldehyde. To investigate this theoretically, a full-dimensional potential energy surface (PES) has been constructed. The PES was fit with permutationally invariant polynomials to 135 000 points calculated using coupled cluster theory with single and double excitations and a perturbative treatment of triple excitations [CCSD(T)] and correlation consistent basis sets of double- and triple- ζ quality. To test the accuracy of the PES additional CCSD(T) and multireference configuration interaction calculations were carried out. Quasiclassical trajectory calculations were run on the PES starting at the acetaldehyde equilibrium geometry and also at the conventional transition state (TS) for the molecular products $\text{CH}_4 + \text{CO}$. The former calculations agree well with the experimental results of Houston and Kable; however, those from the TS do not. The implications for a non-transition state, roaming mechanism in this molecule are discussed.

In a recent report of acetaldehyde photodissociation at 308 nm, Houston and Kable¹ presented experimental evidence of a two-pathway mechanism for formation of $\text{CH}_4 + \text{CO}$. They observed CO with high translational and rotational energy and significant $v_{\perp}L_J$ correlation, consistent with the traditional transition state mechanism. However, they also reported that a significant percentage of the reactions produce CO with low rotational and translational excitation and no $v_{\perp}L_J$ correlation. They speculated, based on similarities with the simpler and well-studied photodissociation of formaldehyde, that these characteristics of the CO rotation are a signature of a component non-transition state, “roaming” dynamics.

The earlier work on formaldehyde to which they referred dates back to experiments by van Zee et al.² where at photolysis energies just below the threshold for the radical $\text{H} + \text{HCO}$, a small shoulder was observed in the experimental CO rotational distribution at lower values of j_{CO} . More recent velocity map imaging experiments together with dynamics calculations on a global potential energy surface (PES) confirmed the earlier speculation by van Zee et al.² that this shoulder was the result of the influence of the $\text{H} + \text{HCO}$ radical channel.^{3,4} In reactions that cause the shoulder, the $\text{H}-\text{C}$ bond is nearly broken, but the H atom cannot quite completely dissociate. The H then undergoes large amplitude roaming motion about the HCO and eventually abstracts the second hydrogen, bypassing the con-

ventional transition state, and forms vibrationally excited H_2 and rotationally cold CO.

There have been numerous ab initio calculations of stationary points relevant to the dissociation of CH_3CHO .^{5–9} The complexity of this system has been demonstrated in detail in very recent work by Yang et al.¹⁰ Direct-dynamics calculations of the dissociation dynamics were reported by Kurosaki¹¹ and Kurosaki and Yokoyama.¹² These calculations (at the MP2/cc-pVDZ level of theory/basis) were initiated at the transition state (TS) saddle point for the $\text{CH}_4 + \text{CO}$ product at a total energy to simulate 248 nm dissociation. The resulting j_{CO} rotational distribution is quite hot with a peak at roughly 60¹¹ or 70,¹² which is much higher than the peak in the colder experimental distribution near 20, obtained at 308 nm.

In this Letter, we report quasiclassical trajectory (QCT) calculations of the dissociation dynamics of CH_3CHO at the energy of the Houston-Kable experiment using a full-dimensional, ab initio-based PES. The QCT calculations were initiated at the global minimum and also, for comparison purposes, from the CH_4-CO TS. The CO rotational distributions and the vector correlations are calculated and compared with experiment.

The ground-state singlet PES was constructed using procedures developed in our group^{13–16} from roughly 135 000 ab initio energies computed with the coupled cluster singles and doubles method with a perturbative treatment of triple excitations [CCSD(T)]. The calculations used the correlation consistent basis sets cc-pVDZ, cc-pVTZ, and aug-cc-pVTZ. The smaller basis set energies were shifted by the difference in energy between the smaller basis sets and the aug-cc-pVTZ basis at the acetaldehyde equilibrium geometry. The CCSD(T) method

* To whom correspondence should be addressed. E-mail: jmbowma@emory.edu.

[†] Department of Chemistry and Cherry L. Emerson Center for Scientific Computation.

[‡] Department of Mathematics and Computer Science.

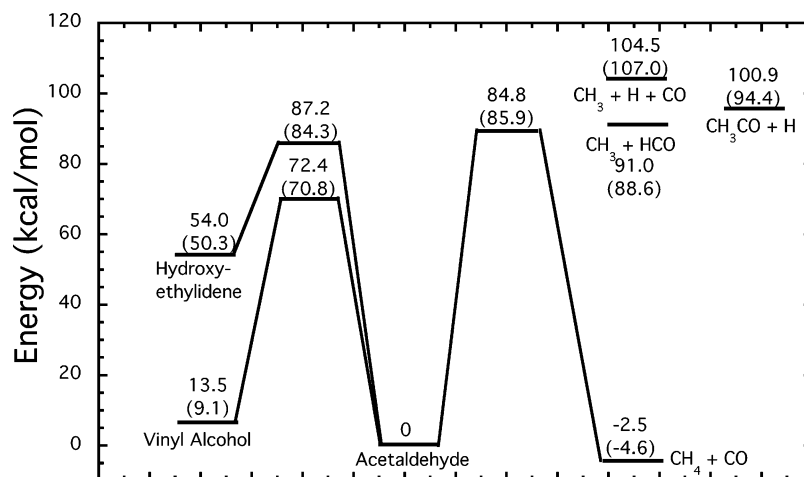


Figure 1. Energy level schematic for selected stationary points on the C_2H_4O PES relative to acetaldehyde equilibrium geometry (kcal/mol). The upper numbers are PES energies at the PES stationary points, and the lower numbers in parenthesis are CCSD(T)/aug-cc-pVTZ energies at the corresponding stationary points. CCSD(T)/aug-cc-pVTZ structures are given in Supporting Information.

properly describes dissociation to the singlet products $CH_4 + CO$; however, it does not properly describe dissociation to radical products like $CH_3 + HCO$. Therefore, no ab initio calculations were carried out in these regions. Reliable CCSD(T) calculations were done for the noninteracting separated radical fragments $CH_3 + HCO$, $CH_3 + H + CO$, $H + CH_3CO$, etc., and it was left to the fit (done using Morse variables and permutationally invariant polynomials in terms of them) to interpolate between the molecular complex and the separated radical fragments. To test that the PES describes these regions correctly, singles and doubles multireference configuration interaction (MRCI) calculations were carried out to confirm the smooth and realistic behavior of the PES for dissociation to radical channels. All calculations were carried out with the MOLPRO suite of electronic structure programs.¹⁷

This system contains numerous minima, saddle points, and fragment channels, and so global fitting is a major challenge. Therefore, to test the robustness of the dynamics calculations two fits were done and used in QCT calculations. These fits were done with polynomial bases of total order 5 and 6. There are 2655 terms in the fifth degree fit and 9953 in the sixth degree fit. As expected for such a complex PES, there are some quantitative differences between these fits and with the ab initio data, for example, energies of some stationary points and separated fragments differ by several kcal/mol. Figure 1 shows a comparison of energies from the fifth order fit with present high-level ab initio calculations for the stationary points and dissociation channels that were found to be important in the QCT calculations. A comparison between direct MRCI calculations and the fifth order PES for cuts leading to $CH_3 + HCO$ and $CH_3CO + H$ is given in Supporting Information, where it can be seen that the fifth order PES does provide a realistic description of dissociation to these radical channels. This fit also contains many other stationary points and fragmentation channels, which will be described in detail in a follow-up paper.

Standard QCT calculations were run on the fifth and sixth order PESs at a total energy corresponding to the 308 nm experiments (92.8 kcal/mol). As in previous QCT calculations for H_2CO ,^{3,4} trajectories were initiated at the CH_3CHO global minimum to avoid biasing the results. The harmonic zero-point energy of CH_3CHO was added giving a total energy of 127.6 kcal/mol. These trajectories are referred to as “equilibrium trajectories” and are denoted as EQ. Random microcanonical sampling of the Cartesian momenta in all degrees of freedom

was done to generate initial conditions subject to the constraint of zero total angular and linear momentum. The time step was 0.12 fs and trajectories were integrated for a maximum of 400 000 time steps (48 ps). This large integration time was necessary for a significant fraction (roughly 3/4) of trajectories to dissociate. Fewer trajectories were run with the sixth order PES owing to the larger CPU time required to use it. For the fifth (sixth) order PES, 8000 (1800) trajectories were run of which roughly 1700 (290) gave $CH_4 + CO$.

A second set of trajectories was initiated at the CH_4-CO TS and “aimed” toward that channel using the same sampling procedures that were done for the EQ trajectories, and as were done previously.^{11,12} We denote these as TS trajectories; they are quite prompt (and can therefore be done with direct dynamics^{11,12}), and so for both the fifth and sixth order PES 6000 TS trajectories were done.

At 308 nm excitation, the energetically open channels are $CH_4 + CO$, $CH_3 + HCO$, $C_2H_2 + H_2O$, $CH_2CO + H_2$, and $H + CH_3CO$. The triple break-up channel, $CH_3 + H + CO$, is closed but only by 2.5 kcal/mol, which is less than the zero-point energy (ZPE) of the products. Thus, in standard QCT calculations, which do not describe the ZPE of products, the channel is open, and in fact roughly 50% of the equilibrium trajectories lead to these products. We dealt with this well-known defect of QCT calculations in the standard way, by discarding those trajectories from the sample. Of the remaining 50% of dissociating trajectories, roughly 30% yield $CH_4 + CO$, 10% yield $CH_3 + HCO$ (some of these are formed with less than ZPE), and another 10% yield other products including H-elimination. $CH_2CO + H_2$ was found as a very minor product and $C_2H_2 + H_2O$ was not observed. Further discussion of these products will be given in a future publication.

The CO rotational distributions from the EQ and TS sets of trajectories run on the fifth and sixth order PESs are compared with the corresponding experimental results of Houston and Kable¹ in Figure 2. The distributions shown are for the dominant ground vibrational state of CO (seen in both experiment and the calculations). The EQ distribution is much colder than the TS one and much closer to experiment. There is much less trajectory data for the $\nu = 1$ and $\nu = 2$ rotational distributions and thus significant statistical noise, but the EQ distributions are in qualitative agreement with the experimental results while the TS distributions are too hot. The distributions from the fifth-

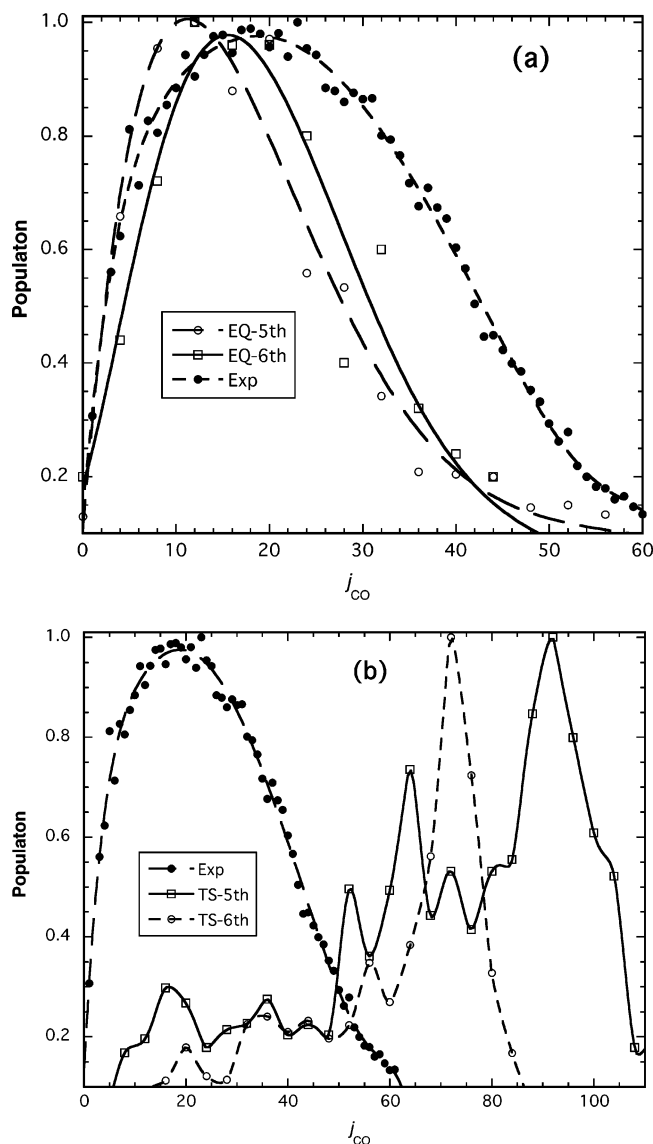


Figure 2. (a) Comparison of experimental (ref 1) CO rotational distribution from 308 nm photolysis of acetaldehyde for CO ($v = 0$) with calculations from equilibrium trajectories initiated at the $\text{CH}_3\text{-CHO}$ minimum, denoted EQ, on the fifth and sixth order PESs; (b) same as (a) but for trajectories initiated at the $\text{CH}_4\text{-CO}$ transition state, denoted TS. The distributions are normalized so that the maximum in each is equal to one. The curves indicated are given to aid in visualization of the results.

and sixth-order EQ trajectories are similar, which provides confidence in the robustness of the present calculations.

We also calculated the internal energy distribution of CH_4 . The EQ and TS results show significant differences with the majority of EQ trajectories giving internal energies greater than 100 kcal/mol and the TS ones giving energies less than 80 kcal/mol. Again, the results from the fifth and sixth order PESs are in semiquantitative accord with each other. Plots of these distributions are given in Supporting Information.

Next consider the vector correlation between the CO rotational vector and the relative translational velocity vector of the CH_4 and CO fragments. In previous direct dynamics TS calculations,¹² it was found that the angle between these vectors was sharply peaked at 90° . By contrast, the experiments of Houston and Kable¹ found that CO with low j_{CO} have little vector correlation, but the opposite was true for highly rotationally excited CO. The calculated vector correlation is shown in Figure 3, where the angle between these vectors as a function

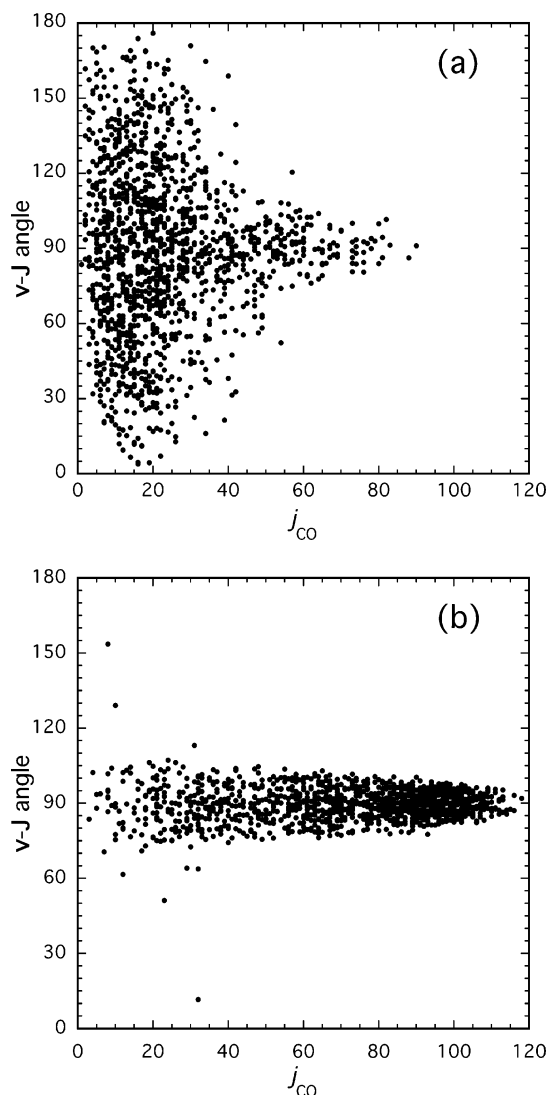


Figure 3. Vector correlation of CO rotational vector (\mathbf{j}) and $\text{CH}_4 + \text{CO}$ relative translational vector (\mathbf{v}). (a) Trajectories initiated at acetaldehyde equilibrium geometry. (b) Trajectories initiated at the conventional transition state.

of j_{CO} is plotted for EQ and TS trajectories. For EQ trajectories, there appears to be almost no correlation for low j_{CO} , but considerable correlation for higher values of j_{CO} in good qualitative agreement with experiment. By contrast, the trajectories initiated at the transition state exhibit strong correlation in disagreement with experiment but in good agreement with the previous direct-dynamics TS calculations.¹²

To sum up thus far, the calculations indicate that non-transition state dynamics play a major role in the photodissociation of acetaldehyde. If reaction flux through the conventional transition state was the dominant mechanism for formation of $\text{CH}_4 + \text{CO}$, the EQ and TS trajectories would be in good agreement with each other, but they are not. They differ significantly in the CO rotational distribution, CH_4 internal energy, and $\mathbf{v} \perp \mathbf{J}$ correlation. Such differences were seen previously in H_2CO (the vector correlation property has been investigated theoretically for H_2CO ¹⁸ but as yet has not been probed experimentally) and like H_2CO suggest two different mechanisms involved in the acetaldehyde photolysis. (Also, it appears that non-TS dynamics may be more significant than the 15% estimate given by Houston and Kable,¹ based on double Gaussian fits to their CO rotational distribution.)

As a first attempt to characterize the non-TS dynamics in the CH_3CHO dissociation, we examined a number of equilibrium trajectories and found several interesting non-TS paths that could all be characterized as roaming. In these trajectories, we see near fragmentation to CH_3 and HCO and also cases of near breakup to $\text{CH}_3 + \text{H} + \text{CO}$ followed in both cases by “abstraction” of the H atom in $\text{H}-\text{CO}$ to form $\text{CH}_4 + \text{CO}$. We also see trajectories that do pass through the conventional TS. On the basis of this examination and simple geometric consideration, it appears that the C–C distance at the “moment” where the H-atom is transferred is a useful and simple metric to distinguish TS and non-TS pathways. We examined this bond length as a function of j_{CO} and find that for j_{CO} less than 45 (which accounts for most of the population of j_{CO} for equilibrium trajectories) the average C–C distance is 3.8 Å with a standard deviation of 0.7 Å, and for j_{CO} greater than 45 this average distance is 2.3 Å with a standard deviation of 0.7 Å. Note that at the conventional saddle point the C–C distance is 2.1 Å, which is quite close to the value we find for $j_{\text{CO}} > 45$. Thus, the conclusion based on our equilibrium trajectories is that for the majority of dissociation events (where j_{CO} is less than 45) the critical geometry where the $\text{CH}_4 + \text{CO}$ are formed the C–C bond distance is almost twice the value at the conventional saddle point. This is consistent with the CH_3-HCO non-TS mechanism proposed by Houston and Kable.¹ This conclusion is also in good accord with the very recent and interesting work of Harding et al. who report a very floppy roaming TS for the $\text{CH}_4 + \text{CO}$ products where the C–C distance is 3.4 Å.⁶ (Indeed, we were stimulated to consider the C–C distance as a metric based on the results in that paper and in private communication with Harding.)

Future work will focus on improving the description of the potential energy surface, including extensive multireference calculations and more data points and additional dynamics calculations. However, the insensitivity of the dynamics calculations to the two different surfaces used here and the agreement between the equilibrium trajectories and experiment support the robustness of the current results.

Acknowledgment. B.C.S. thanks the National Science Foundation (CHE-0625237), B.J.B. thanks the Office of Naval Research (N00014-05-1-0460), and J.M.B. thanks the Department of Energy (DE-FG02-97ER14782) for financial support. This work was also partially supported by the National Center for Supercomputing Center for Supercomputing Applications

under Grant CHE-060071, and the Tungsten computer cluster was used. The research also used resources of the National Energy Research Scientific Computing Center, which is supported by the Office of Science of the U.S. Department of Energy under Contract No. DE-AC02-05CH11231. We thank Larry Harding for sending a preprint of ref 6 and Scott Kable and Paul Houston for sending their experimental data.

Supporting Information Available: Comparison of 1d cuts from PES and MRCI+Q calculations, CH_4 internal energy distributions versus CO rotational quantum number, and optimized structures. This material is available free of charge via the Internet at <http://pubs.acs.org>.

References and Notes

- (1) Houston, P. L.; Kable, S. H. *Proc. Natl. Acad. Sci. U.S.A.* **2006**, *103*, 16079.
- (2) van Zee, R. D.; Foltz, M. F.; Moore, C. B. *J. Chem. Phys.* **1993**, *99*, 1664.
- (3) Townsend, D.; Lahankar, S. A.; Lee, S. K.; Chambreau, S. D.; Suits, A. G.; Zhang, X.; Rheinecker, J.; Harding, L. B.; Bowman, J. M. *Science* **2004**, *306*, 1158.
- (4) Zhang, X.; Rheinecker, J.; Bowman, J. M. *J. Chem. Phys.* **2005**, *122*, 114313.
- (5) Gherman, B. F.; Friesner, R. A.; Wong, T. H.; Min, Z.; Bersohn, R. *J. Chem. Phys.* **2001**, *114*, 6128.
- (6) Harding, L. B.; Klippenstein, S. J.; Jasper, A. W. *Phys. Chem. Chem. Phys.* **2007**, *9*, 1.
- (7) Martell, J. M.; Yu, H.; Goddard, J. D. *Mol. Phys.* **1997**, *92*, 497.
- (8) Smith, B. J.; Nguyen, M. T.; Bouma, W. J.; Radom, L. *J. Am. Chem. Soc.* **1991**, *113*, 6452.
- (9) Yadav, J. S.; Goddard, J. D. *J. Chem. Phys.* **1986**, *84*, 2682.
- (10) Yang, X.; Maeda, S.; Ohno, K. *J. Phys. Chem. A* **2007**, *111*, 5099.
- (11) Kurosaki, Y. *Chem. Phys. Lett.* **2006**, *421*, 549.
- (12) Kurosaki, Y.; Yokoyama, K. *J. Phys. Chem. A* **2002**, *106*, 11415.
- (13) Brown, A.; Braams, B. J.; Christoffel, K.; Jin, Z.; Bowman, J. M. *J. Chem. Phys.* **2003**, *119*, 8790.
- (14) Huang, X.; Braams, B. J.; Carter, S.; Bowman, J. M. *J. Am. Chem. Soc.* **2004**, *126*, 5042.
- (15) Park, S. C.; Braams, B. J.; Bowman, J. M. *J. Theor. Comp. Chem.* **2005**, *4*, 163.
- (16) Xie, Z.; Braams, B. J.; Bowman, J. M. *J. Chem. Phys.* **2005**, *122*, 224307.
- (17) Amos, A.; Bernhardsson, A.; Berning, A.; Celani, P.; Cooper, D. L.; Deegan, M. J. O.; Dobbyn, A. J.; Eckert, F.; Hampel, C.; Hetzer, G.; Knowles, P. J.; Korona, T.; Lindh, R.; Lloyd, A. W.; McNicholas, S. J.; Manby, F. R.; Meyer, W.; Mura, M. E.; Nicklass, A.; Palmieri, P.; Pitzer, R.; Rauhut, G.; Schütz, M.; Schumann, U.; Stoll, H.; Stone, A. J.; Tarroni, R.; Thorsteinsson, T.; Werner, H.-J. *MOLPRO*, version 2002.6. *MOLPRO* is a package of ab initio programs written by H.-J. Werner and P. J. Knowles. <http://www.molpro.net>.
- (18) Farnum, J. D.; Zhang, X.; Bowman, J. M. *J. Chem. Phys.* **2007**, *126*, 134305.